Molecular dynamics study of phase separation in fluids with chemical reactions

Raishma Krishnan and Sanjay Puri
School of Physical Sciences, Jawaharlal Nehru University, New Delhi 110067, India
(Received 11 March 2015; revised manuscript received 10 September 2015; published 30 November 2015)

We present results from the first $d = 3$ molecular dynamics (MD) study of phase-separating fluid mixtures (AB) with simple chemical reactions (A $\rightleftharpoons$ B). We focus on the case where the rates of forward and backward reactions are equal. The chemical reactions compete with segregation, and the coarsening system settles into a steady-state mesoscale morphology. However, hydrodynamic effects destroy the lamellar morphology which characterizes the diffusive case. This has important consequences for the phase-separating structure, which we study in detail. In particular, the equilibrium length scale ($\ell_{\rm eq}$) in the steady state suggests a power-law dependence on the reaction rate ϵ: $\ell_{\rm eq} \sim \epsilon^{-\theta}$ with $\theta \simeq 1.0$.

DOI: 10.1103/PhysRevE.92.052316 PACS number(s): 64.75.Va, 64.60.De, 64.70.Ja

I. INTRODUCTION

In recent years, there has been great interest in the phase-separation kinetics of a binary mixture (AB), which has been destabilized by a quench from a high-temperature homogeneous state to a point below the coexistence curve at time $t = 0$ [1–3]. This thermodynamically unstable system evolves via the emergence and growth of A-rich and B-rich domains, which are characterized by a single time-dependent length scale $\ell(t)$. Such systems have been extensively studied through experiments, numerical simulations, and approximate analytical methods [1–3].

It is now well established that domain growth or coarsening is a scaling phenomenon. The *correlation function* $C(\vec{r},t)$, where $\vec{r}$ is the separation between two points, exhibits *dynamical scaling*: $C(\vec{r},t) = g[r/\ell(t)]$. Similarly, the *structure factor* $S(\vec{k},t)$, which is the Fourier transform of $C(\vec{r},t)$ at wave vector $\vec{k}$, obeys $S(\vec{k},t) = \ell(t)^d f[k\ell(t)]$. Here $g(x)$ and $f(p)$ are scaling functions, and d is the spatial dimensionality. In many systems, $\ell(t)$ has a simple power-law dependence on time: $\ell(t) \sim t^{\phi}$, where ϕ is the *growth exponent*. The value of ϕ depends on the physical mechanisms controlling domain growth.

Many experiments on phase separation are performed on fluid or polymer mixtures. Segregating fluids are characterized by several different growth regimes, e.g., for $d = 3$:

$$\begin{aligned}\ell(t) &\sim (D\sigma t)^{1/3}, \quad \ell \ll (D\eta)^{1/2} \\ &\quad (\textit{diffusive or Lifshitz-Slyozov regime}) \\ &\sim \frac{\sigma t}{\eta}, \quad (D\eta)^{1/2} \ll \ell \ll \frac{\eta^2}{\rho\sigma} \\ &\quad (\textit{viscous hydrodynamic regime}) \\ &\sim \left(\frac{\sigma t^2}{\rho}\right)^{1/3}, \quad \frac{\eta^2}{\rho\sigma} \ll \ell \\ &\quad (\textit{inertial hydrodynamic regime}). \end{aligned} \tag{1}$$

In Eq. (1), D denotes the diffusion coefficient; σ is the surface tension; η is the viscosity; and ρ is the density. The diffusive regime has been observed in many numerical studies [4–6]. The viscous hydrodynamic regime has also been observed in many simulations. These include studies of coarse-grained models like *Model H* or its variants [7–9]. However, it has proven harder to observe the linear growth regime with microscopic-level molecular dynamics (MD) models, where hydrodynamic effects are naturally included. An unambiguous confirmation of this regime has only been provided by the recent MD simulations of Ahmad *et al.* [10]. Finally, the inertial regime with $\ell \sim t^{2/3}$ has only been observed numerically in *lattice Boltzmann* simulations [11,12], which are analogous to coarse-grained models. To date, MD simulations have not accessed the inertial growth regime as this is computationally very demanding [10].

In this paper, we study phase separation in chemically reactive fluid mixtures. These systems have been experimentally realized by Tran-Cong and others, who showed that mesoscale morphologies arise when chemical reactions are photoinduced in segregating polymers. This group has studied two classes of photochemical processes: *intermolecular dimerization* [13] and *intramolecular isomerization* [14]. There have also been some earlier numerical studies of this problem, but these have primarily focused on the case with diffusive transport. We will shortly review some of these works. As discussed above, hydrodynamic effects in fluid mixtures drastically alter the late stages of segregation kinetics. It is experimentally relevant to ask how chemical reactions affect the crossover scenario of phase-separating fluids. In this paper, we undertake the first three-dimensional (3D) MD simulation of segregation with chemical reactions. As stated earlier, MD techniques have the advantage of naturally incorporating hydrodynamic effects.

Let us start by briefly reviewing some earlier studies of this problem. The first studies are due to Puri and Frisch (PF) [15,16] and Glotzer *et al.* [17–19]. PF modified the Cahn-Hilliard (CH) equation for diffusion-driven phase separation by including simple chemical reactions: A $\rightleftharpoons$ B, AB $\rightleftharpoons$ BB, etc. For the reaction A $\rightleftharpoons$ B, they formulated the following model (in dimensionless units):

$$\frac{\partial \psi(\vec{r},t)}{\partial t} = -\nabla^2(\psi - \psi^3 + \nabla^2\psi) - \alpha\psi - \beta, \tag{2}$$

where $\psi(\vec{r},t)$ is the order-parameter field (density difference of A and B) as a function of space $\vec{r}$ and time t. The parameters α and β depend on the rates of the forward reaction $\epsilon_1 = \tau_1^{-1}$ and backward reaction $\epsilon_2 = \tau_2^{-1}$: $\alpha \sim \epsilon_1 + \epsilon_2$; $\beta \sim \epsilon_1 - \epsilon_2$. For the interesting case where $\epsilon_1 = \epsilon_2$, we have $\beta = 0$ in Eq. (2). PF pointed out that Eq. (2) is the same as the model proposed and studied by Oono-Shiwa [20] and

Oono-Bahiana [21,22] in the unrelated context of microphase separation in block copolymers (BCPs) of the form A_nB_m. In BCPs, the nonconserving term on the RHS of Eq. (2) arises from a long-ranged repulsive interaction term in the free energy. The coarsening BCP freezes into a microdomain morphology dictated by the relative lengths $(n:m)$ of the copolymer, e.g., lamellae, gyroids, cylinders, spheres, etc. The case of a symmetric BCP $(n=m)$ is analogous to the case $\epsilon_1=\epsilon_2$ and results in a lamellar morphology.

The same problem was independently studied by Glotzer *et al.* (GSJ) [17] via Monte Carlo (MC) simulations. GSJ studied an Ising model with Kawasaki spin-exchange kinetics (modeling diffusive phase separation [1]) in conjunction with the chemical reaction A $\rightleftharpoons$ B, with $\epsilon_1=\epsilon_2=\epsilon$. They showed that the coarsening system freezes into a lamellar morphology with a length scale $\ell_{\rm eq}\sim\epsilon^{-\theta}(\theta\simeq 0.22)$. In subsequent work, Glotzer *et al.* (GMM) [19] studied the linear instability and long-time kinetics of Eq. (2) in the limit $\beta=0(\epsilon_1=\epsilon_2=\epsilon)$. Again, they found that the system settles into a lamellar morphology with $\ell_{\rm eq}\sim\epsilon^{-\theta}$, where $\theta\simeq 0.33$. Notice that this exponent is the same as the Lifshitz-Slyozov growth exponent $(\phi=1/3)$, which characterizes diffusive phase separation [21,22]. This result was later confirmed by more comprehensive simulations of Eq. (2) by Christensen *et al.* [23]. In this context, an interesting work is due to Kuksenok *et al.* [24], who used coupled CH equations to study phase-separating ternary mixtures with chemical reactions.

So far, we have been discussing diffusion-driven phase separation. It is natural to query how hydrodynamics affects the above picture, particularly as most experiments on segregation are performed in fluid or polymer mixtures. In the absence of chemical reactions, we have already stressed that phase-separating fluids show a crossover in the growth exponent, $1/3\rightarrow 1\rightarrow 2/3$, as in Eq. (1). An early MD simulation (in $d=2$) of phase separation with chemical reactions (A $\rightleftharpoons$ B) is due to Toxvaerd [25]. He argued that the coarsening system freezes into a steady state but the velocity field destroys the lamellar structure. However, we should stress that two-dimensional (2D) hydrodynamics suffers from some physical problems, e.g., several transport coefficients are divergent. Next, we mention the study of Huo *et al.* (HJZ) [26], who studied a modified version of Model H. HJZ incorporated the chemical reaction A $\rightleftharpoons$ B by including a long-range interaction term (as in BCPs) in the free-energy functional. This term was only included in the kinetic equation for $\psi(\vec{r},t)$ and was absent from the Navier-Stokes equation for the velocity field $\vec{v}(\vec{r},t)$, which appears to be physically inconsistent. Further, their 2D simulation of Model H was complicated by the observation of *double phase separation*. Therefore, it is unclear what reliable statements the HJZ simulation makes about "phase separation in fluids with chemical reactions."

Finally, we mention a 2D lattice Boltzmann (LB) simulation of this problem by Furtado and Yeomans (FY) [27]: the LB model is analogous to Model H. FY solved the modified CH equation in conjunction with the LB equations for conservation of mass and momentum. They studied both the linear reaction A $\rightleftharpoons$ B and the quadratic reaction A +B $\rightleftharpoons$ 2B [15,16]. For the linear reaction, FY found that the lamellar structure survived in the presence of hydrodynamics at high reaction rates. However, regions of very high interfacial curvature are eliminated by the flow field. FY did not make any quantitative statements about the dependence of the steady-state domain scale on the reaction rate.

From the above discussion, it is clear that we have a poor understanding of segregating fluids with chemical reactions. In this paper, we report a 3D MD simulation of this problem. As mentioned above, the MD approach naturally incorporates flow fields. However, MD simulations are computationally very demanding, and this has proven an obstacle in their widespread usage. This paper is organized as follows. In Sec. II, we provide details of our MD simulations. In Sec. III, we present comprehensive numerical results. Finally, in Sec. IV, we conclude with a summary and discussion.

II. DETAILS OF MOLECULAR DYNAMICS SIMULATIONS

For our MD simulations, we consider a fluid mixture with equal numbers of A and B particles $(N_A=N_B=N/2)$ confined in a volume $V=(L_s\sigma)^3$ [10,28]. The particles have equal masses $(m_A=m_B=m=1)$ and diameters $(\sigma_A=\sigma_B=\sigma=1)$. They interact via the Lennard-Jones (LJ) pairwise potential:

$$V_{\rm LJ}(r)=4\epsilon_{\alpha\beta}\left[\left(\frac{\sigma}{r}\right)^{12}-\left(\frac{\sigma}{r}\right)^{6}\right], \tag{3}$$

where $r=|\vec{r}_i-\vec{r}_j|$ and $\alpha,\beta=A,B$. We take the energy scales as $\epsilon_{AA}=\epsilon_{BB}=2\epsilon_{AB}=\epsilon_0$. This corresponds to a symmetric binary mixture, whose equilibrium phase diagram is well understood [29,30]. For our simulations, we use the truncated, shifted, and force-corrected LJ potential:

$$\begin{aligned} U(r) &= V_{\rm LJ}(r)-V_{\rm LJ}(r_c)-(r-r_c)\left.\frac{dV_{\rm LJ}}{dr}\right|_{r=r_c}, \quad r<r_c \\ &= 0, \quad r>r_c, \end{aligned} \tag{4}$$

with the cutoff $r_c=2.5\sigma$ [31,32]. We work in the high-density liquid regime, $\rho^*=N\sigma^3/V=1$, and hence the system is incompressible. We also set $\epsilon_0=1$ and $k_B=1$, such that the dimensionless MD time unit is

$$t_0=\left(\frac{m\sigma^2}{\epsilon_0}\right)^{1/2}=1. \tag{5}$$

We consider a total number of $N=110\,592$ particles confined in a cubic box of size 48^3, with periodic boundary conditions in all directions. The MD runs were carried out using the standard *velocity Verlet algorithm* [33] with a time step $\Delta t=0.01t_0$. The temperature T is maintained constant via the Nosé-Hoover thermostat, which is known to preserve hydrodynamics [10,33].

The homogeneous initial state for a run is prepared by equilibrating the system at a high temperature $(T=5)$ for 2×10^5 MD steps. At time $t=0$, the system is quenched to $T=1.0\simeq 0.77T_c$ ($T_c\simeq 1.423$ in $d=3$ [29,30]). This temperature is well separated from the gas-liquid and liquid-solid transitions in this system. All statistical results presented here are obtained by averaging over 10 independent runs.

The chemical reaction A $\rightleftharpoons$ B is incorporated by randomly choosing a particle (A or B) and changing its label, i.e., A $\rightarrow$ B and B $\rightarrow$ A. The chemical reaction tends to mix the two species, thereby opposing phase separation. We considered

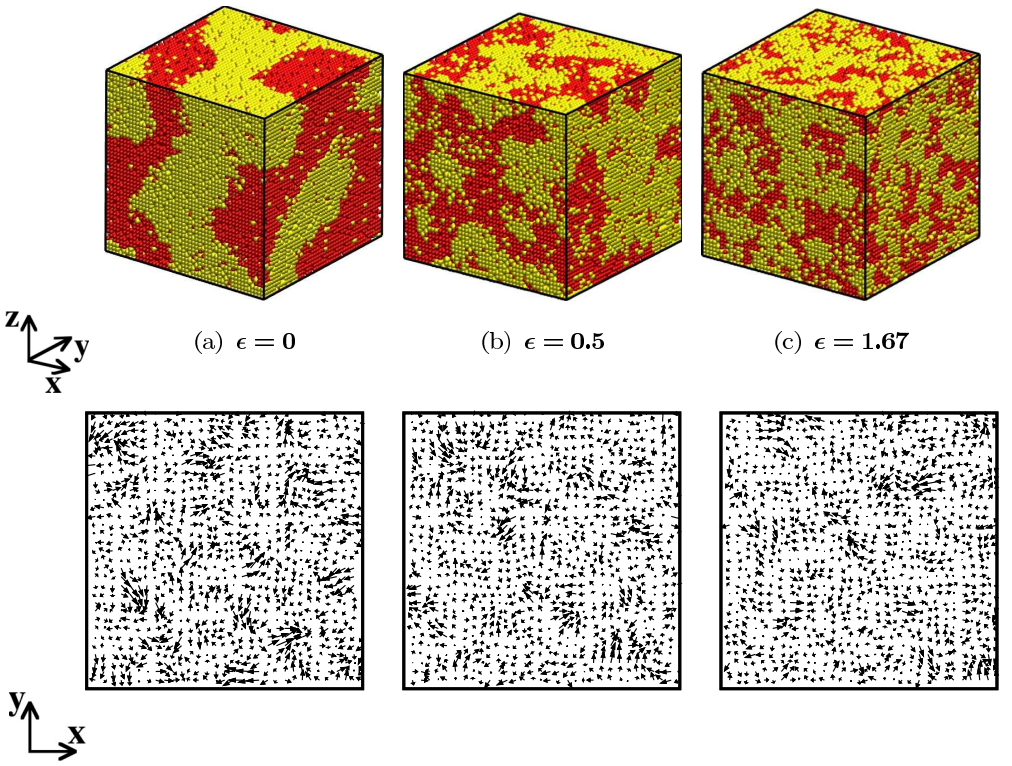

FIG. 1. (Color online) Evolution snapshots (upper frames) of a chemically reactive binary mixture (AB) at $t = 21\,000$ for reaction rates $\epsilon = 0,0.5,1.67$. The A-rich and B-rich regions are marked red (black) and yellow (gray), respectively. The lower frames show the corresponding velocity fields (v_x,v_y) in the (xy) plane for the layer $z \in [4.5,6]$.

five different rates, namely, $\epsilon = 1/6,1/2,1,5/3$, and 5. To obtain the rate $\epsilon = 5/3$, say, five particles are changed every three MD steps. We compared the evolution for different values of ϵ to the case without a reaction ($\epsilon = 0$). The quantities that characterize the evolution morphologies are (a) the time-dependent correlation function $C(\vec{r},t)$ and structure factor $S(\vec{k},t)$; and (b) the characteristic length scale $\ell(t)$. The structure factor is the quantity monitored in most experiments like neutron or light scattering. If the system is characterized by a single length scale $\ell(t)$, the morphology of the domains does not change with time, apart from a scale factor.

The order-parameter correlation function is computed as

$$C(\vec{r},t) = \langle\psi(\vec{r}_1,t)\psi(\vec{r}_2,t)\rangle - \langle\psi(\vec{r}_1,t)\rangle\langle\psi(\vec{r}_2,t)\rangle, \quad (6)$$

where $\vec{r} = \vec{r}_2 - \vec{r}_1$. The angular brackets in Eq. (6) denote statistical averaging over independent runs. (A similar definition applies for the correlation function of the velocity field, which we denote as C_v.) To obtain the order parameter $\psi(\vec{r},t)$, we use a coarse-graining procedure which is the numerical counterpart of the renormalization group (RG) technique [34]. Our system is first divided into nonoverlapping boxes of size $\lambda^3 = (1.5\sigma)^3$. We then count the total number of A and B particles in each box, say, n_A and n_B. If $n_A > n_B$, we set $\psi = +1$. On the other hand, if $n_A < n_B$, we set $\psi = -1$. However, when $n_A = n_B$, we assign $+1$ or -1 randomly. This coarse-graining procedure helps us to obtain the domain structure devoid of thermal fluctuations. Our statistical results do not have a sensitive dependence upon the coarse-graining scale λ. We require $\lambda > 1$ so that each box contains a reasonable number of particles. Further, it is convenient to choose $(L_s\sigma)/\lambda$ as a power of two so that we can use *fast Fourier transforms* to evaluate $C(\vec{r},t)$ and $S(\vec{k},t)$. To improve the statistics, we spherically average $C(\vec{r},t)$ and $S(\vec{k},t)$ to obtain the isotropic functions $C(r,t)$ and $S(k,t)$. The average domain size $\ell(t)$ is defined as the first zero crossing of $C(r,t)$.

III. NUMERICAL RESULTS

In Fig. 1 we present the evolution snapshots (upper frames) of a chemically reactive fluid mixture at $t = 21\,000$ for $\epsilon = 0,0.5,1.67$. The snapshots show that the chemical reaction slows segregation. We will shortly see that the system settles into a steady state. However, we find no evidence of the lamellar structures reported in the LB studies of FY [27]. Our results show that hydrodynamic effects destroy the lamellar structures which are observed in the diffusive case. This should be contrasted with the closely related BCP segregation problem, where the diffusive model is identical to that for segregation with chemical reactions. The recent MD simulations of BCP segregation by Singh *et al.* [35] show that the steady-state lamellar morphology survives in the presence of hydrodynamics.

The lower frames of Fig. 1 show 2D cross sections of the corresponding velocity field. We compute the velocity field $\vec{v}(\vec{r},t) = (v_x,v_y,v_z)$ by summing over all particles in cubes of size $(1.5\sigma)^3$. The vectors in Fig. 1 denote the direction and magnitude of (v_x,v_y) for $z \in [4.5,6]$. In earlier work, Ahmad *et al.* [10] have stressed that the velocity field in MD simulations of phase-separating mixtures ($\epsilon = 0$ case) is characterized by vortex or antivortex defects, but these do

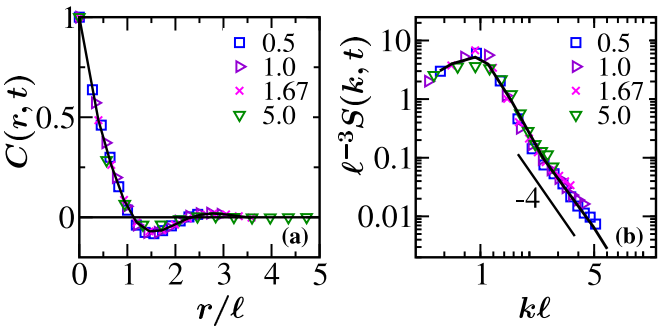

FIG. 2. (Color online) Scaling plots of density correlation functions and structure factors at $t = 21\,000$ for reaction rates $\epsilon = 0.5, 1.0, 1.67, 5.0$. The length scale ℓ is defined as the first zero crossing of $C(r,t)$. The solid lines denote the corresponding data for $\epsilon = 0$ (no chemical reaction). (a) $C(r,t)$ vs r/ℓ; (b) $\ell^{-3}S(k,t)$ vs $k\ell$.

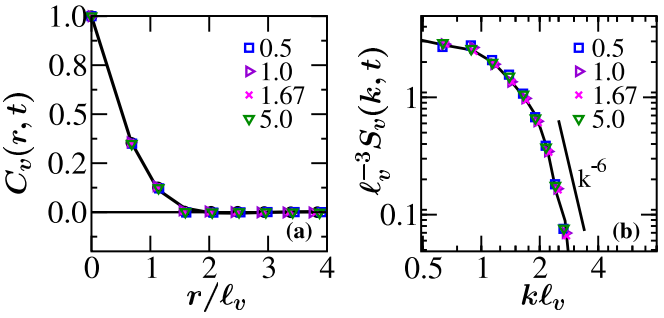

FIG. 3. (Color online) Scaling plots of velocity correlation functions and structure factors at $t = 21\,000$ for reaction rates $\epsilon = 0.5, 1.0, 1.67, 5.0$. The length scale ℓ_v is defined as the distance over which $C_v(r,t)$ falls to 0.1. The solid lines denote the corresponding data for $\epsilon = 0$. (a) $C_v(r,t)$ vs r/ℓ_v; (b) $\ell_v^{-3}S_v(k,t)$ vs $k\ell_v$.

not show a marked coarsening. In the present study, we find that the velocity field is not affected by the chemical reaction. It does not show major differences for the cases with $\epsilon = 0$ and $\epsilon \neq 0$ in Fig. 1, as we will see shortly.

For each value of ϵ, we have confirmed that $C(r,t)$ and $S(k,t)$ obey dynamical scaling for different times. This is checked by superposing data for $C(r,t)$ versus r/ℓ and $\ell^{-d}S(k,t)$ versus $k\ell$ from several different times. In the diffusive case, dynamical scaling breaks down due to a crossover from a bicontinuous morphology at early times to a lamellar morphology at later times. The lamellar morphology is characterized by oscillations in $C(r,t)$ and a marked shoulder in $S(k,t)$ [35]. However, in the present case, the velocity field destroys the lamellar structure. Therefore, the chemically reacting fluid mixture is characterized by the usual bicontinuous structure of segregating systems. This is confirmed in Fig. 2(a), where we plot $C(r,t)$ versus r/ℓ at $t = 21\,000$ for $\epsilon = 0, 0.5, 1.0, 1.67, 5.0$. The scaling function is independent of the value of ϵ and is comparable to that for $\epsilon = 0$. In Fig. 2(b), we present a scaling plot of the structure factor: $\ell^{-d}S(k,t)$ versus $k\ell$ at $t = 21\,000$ for the same values of ϵ as in Fig. 2(a). Again, we see that the scaling function is independent of ϵ. A notable feature of $S(k,t)$ is the Porod tail, $S(k,t) \sim k^{-(d+1)}$, which results from scattering off sharp interfaces.

In Fig. 3(a) we plot the correlation function of the velocity field: $C_v(r,t)$ versus r/ℓ_v. In this case, ℓ_v is defined as the distance over which $C_v(r,t)$ decays to 0.1. We present data for several values of ϵ at $t = 21\,000$. The scaling functions are numerically coincident, confirming that the morphology and length scale of the velocity field is independent of the chemical reaction. The corresponding scaling plot for the structure factor, $\ell_v^{-d}S_v(k,t)$ versus $k\ell_v$, is shown in Fig. 3(b). Notice that the tail shows a generalized Porod behavior, $S_v(k,t) \sim k^{-(d+n)}$, where $n = 3$ for the three-component velocity field. This was first predicted by Bray and Puri [36] in the context of domain growth with a vector order parameter.

Let us return to our discussion of the density field. We focus next on the time dependence of the domain scale. In Fig. 4 we plot $\ell(t)$ versus t on a log-log scale for several values of ϵ, including $\epsilon = 0$ (no chemical reaction) for reference. For $\epsilon = 0$, we expect a power-law domain growth: $\ell \sim t^{\phi}$ with crossovers as $\phi = 1/3 \to 1 \to 2/3$. As mentioned earlier, the $t^{2/3}$-regime has yet to be observed in MD simulations as this requires a huge computational effort [10]. Our $\epsilon = 0$ data in Fig. 4 show the $t^{1/3}$ and t^{1} regimes clearly. At very late stages, there is a crossover to a slower regime than t^{1}, which may be the first MD evidence for $t^{2/3}$ inertial hydrodynamic growth. However, this must be confirmed by longer runs with larger system sizes. As expected, the chemical reaction slows domain growth. There is an early-time window where the data for $\epsilon \neq 0$ are comparable to that for the nonreacting mixture. This is followed by a crossover to slower growth, with crossover time $t_c \sim \epsilon^{-1}$. The slower growth culminates in a steady state with a constant length scale $\ell_{\rm eq}$. Notice that the ℓ values in Fig. 4 do not exceed $\ell_{\rm max} \simeq 5$, which is approximately 10% of the lateral system size ($L_s = 48$). Therefore, we do not expect finite-size effects to be relevant at these length scales [4]. In Fig. 4 we see this freezing for $\epsilon = 1.0, 1.67, 5.0$. We need larger systems and longer runs, which are computationally very expensive, to access the steady states for $\epsilon = 0.17, 0.5$.

In Fig. 5 we plot $\ell_{\rm eq}^{-1}$ versus ϵ. [We approximate $\ell_{\rm eq}$ by $\ell(21\,000)$, which is an underestimate for $\epsilon = 0.17, 0.5$.]We do

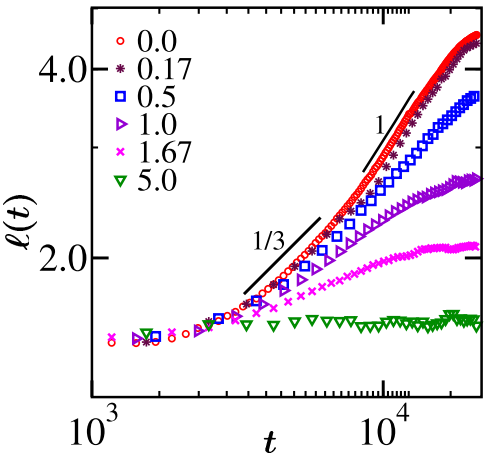

FIG. 4. (Color online) Time dependence of the domain length scale, $\ell(t)$ vs t, for $\epsilon = 0, 0.17, 0.5, 1.0, 1.67, 5.0$. The lines of slope 1/3 and 1 denote the *diffusive* and *viscous hydrodynamic* regimes, respectively.

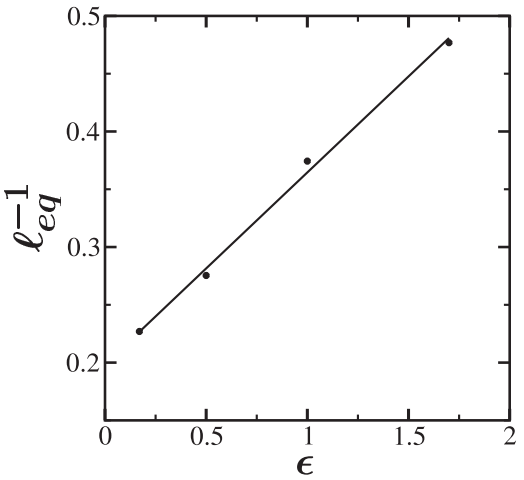

FIG. 5. Equilibrium length scale, $\ell_{\rm eq}^{-1}$ vs ϵ, for the evolution shown in Fig. 4. We approximate $\ell_{\rm eq}$ by $\ell(21\,000)$. The solid line denotes the best linear fit to the data set.

not show the data for $\epsilon = 5.0$, as $\ell_{\rm eq} \sim O(1)$ in that case. Thus, it is comparable to the microscopic length scale and cannot be reliably obtained. The equilibrium length scale suggests a power-law behavior with $\ell_{\rm eq}^{-1} \sim \epsilon^{\theta}$, where $\theta \simeq 1.0$. However, better-quality data for more values of ϵ are needed for an unambiguous confirmation of this behavior. Recall that the corresponding value of θ in the diffusive case is $\theta \simeq 0.33$, which is the same as the growth exponent ϕ for diffusion-driven phase separation. The identification $\theta = \phi$ in the diffusive case generalizes to the case with hydrodynamics.

IV. SUMMARY AND DISCUSSION

Let us conclude this paper with a summary and discussion. We have presented results from the first 3D MD simulation of phase-separation kinetics in chemically reacting fluid mixtures (AB). We consider the simple reaction A $\rightleftharpoons$ B (with equal rates of backward and forward reactions), realized in the experiments of Tran-Cong and others [13,14]. We find that the hydrodynamic velocity field destroys the lamellar structures which characterize the steady state in the diffusive case. For this reason, the evolution morphologies in our MD simulations are characterized by dynamical scaling. (Notice that this breaks down in the diffusive case because of the crossover from an early-time bicontinuous morphology to an asymptotically lamellar morphology [35].) The equilibrium length in the steady-state suggests a power-law scaling with the reaction rate: $\ell_{\rm eq} \sim \epsilon^{-\theta}$ with $\theta \simeq 1.0$.

In general, chemical reactions induced by external agents provide a simple means of controlling the morphology of phase-separating systems, as it is possible to adjust the reaction rates in experiments [13,14]. A typical example of a system undergoing the kind of reaction considered here is the dissociation of a radioactive atom A into a daughter atom B. We believe that the MD results presented here will motivate further experimental and theoretical interest in this problem.

ACKNOWLEDGMENTS

R.K. gratefully acknowledges Department of Science and Technology (India) for financial support through the DST fast-track projects: SR/FTP/PS-12/2009 and SR/FTP/PS-42/2012. S.P. is also grateful to DST for support through a J. C. Bose fellowship.

[1] S. Puri and V. K. Wadhawan (eds.), *Kinetics of Phase Transitions* (CRC Press, Boca Raton, FL, 2009).
[2] K. Binder, in *Phase Transformation of Materials*, edited by R. W. Cahn, P. Haasen, and E. J. Kramer, Material Science and Technology (VCH, Weinheim, 1991), Vol. 5, p. 405.
[3] A. J. Bray, Adv. Phys. **43**, 357 (1994).
[4] Y. Oono and S. Puri, Phys. Rev. Lett. **58**, 836 (1987).
[5] Y. Oono and S. Puri, Phys. Rev. A **38**, 434 (1988).
[6] S. Puri and Y. Oono, Phys. Rev. A **38**, 1542 (1988).
[7] T. Koga and K. Kawasaki, Phys. Rev. A **44**, R817 (1991).
[8] S. Puri and B. Dunweg, Phys. Rev. A **45**, R6977 (1992).
[9] A. Shinozaki and Y. Oono, Phys. Rev. Lett. **66**, 173 (1991); Phys. Rev. E **48**, 2622 (1993).
[10] S. Ahmad, S. K. Das, and S. Puri, Phys. Rev. E **82**, 040107(R) (2010); **85**, 031140 (2012).
[11] V. M. Kendon, J. C. Desplat, P. Bladon, and M. E. Cates, Phys. Rev. Lett. **83**, 576 (1999).
[12] V. M. Kendon, M. E. Cates, I. Pagonabarraga, J. C. Desplat, and P. Blandon, J. Fluid Mech. **440**, 147 (2001).
[13] Q. Tran-Cong and A. Harada, Phys. Rev. Lett. **76**, 1162 (1996); Q. Tran-Cong, A. Harada, K. Kataoka, T. Ohta, and O. Urakawa, Phys. Rev. E **55**, R6340 (1997).
[14] Q. Tran-Cong, T. Ohta, and O. Urakawa, Phys. Rev. E **56**, R59(R) (1997); T. Ohta, O. Urakawa, and Q. Tran-Cong, Macromolecules **31**, 6845 (1998).
[15] S. Puri and H. L. Frisch, J. Phys. A **27**, 6027 (1994).
[16] S. Puri and H. L. Frisch, Int. J. Mod. Phys. B **12**, 1623 (1998).
[17] S. C. Glotzer, D. Stauffer, and N. Jan, Phys. Rev. Lett. **72**, 4109 (1994).
[18] S. C. Glotzer, in *Annual Reviews of Computational Physics*, edited by D. Stauffer (World Scientific, Singapore, 1995), Vol. II, p. 1.
[19] S. C. Glotzer, E. A. Di Marzio, and M. Muthukumar, Phys. Rev. Lett. **74**, 2034 (1995).
[20] Y. Oono and Y. Shiwa, Mod. Phys. Lett. B **1**, 49 (1987).
[21] Y. Oono and M. Bahiana, Phys. Rev. Lett. **61**, 1109 (1988).
[22] M. Bahiana and Y. Oono, Phys. Rev. A **41**, 6763 (1990).
[23] J. J. Christensen, K. Elder, and H. C. Fogedby, Phys. Rev. E **54**, R2212 (1996).
[24] O. Kuksenok, R. D. M. Travasso, and A. C. Balazs, Phys. Rev. E **74**, 011502 (2006).
[25] S. Toxvaerd, Phys. Rev. E **53**, 3710 (1996).
[26] Y. Huo, X. Jiang, H. Zhang, and Y. Yang, J. Chem. Phys. **118**, 9830 (2003).
[27] K. Furtado and J. M. Yeomans, Phys. Rev. E **73**, 066124 (2006).
[28] S. K. Das, S. Puri, J. Horbach, and K. Binder, Phys. Rev. Lett. **96**, 016107 (2006); Phys. Rev. E **73**, 031604 (2006).
[29] S. Roy and S. K. Das, Europhys. Lett. **94**, 36001 (2011).

[30] S. K. Das, J. Horbach, K. Binder, M. E. Fisher, and J. V. Sengers, J. Chem. Phys. **125**, 024506 (2006).
[31] M. P. Allen and D. J. Tildesley, *Computer Simulation of Liquids* (Clarendon Press, Oxford, 1987).
[32] D. Frenkel and B. Smit, *Understanding Molecular Simulations: From Algorithms to Applications* (Academic, San Diego, 2002).
[33] K. Binder and G. Ciccotti (eds.), *Monte Carlo and Molecular Dynamics of Condensed Matter Systems* (Italian Physical Society, Bologna, 1996).
[34] S. K. Das and S. Puri, Phys. Rev. E **65**, 026141 (2002).
[35] A. Singh, R. Krishnan, and S. Puri, Europhys. Lett. **109**, 26006 (2015).
[36] A. J. Bray and S. Puri, Phys. Rev. Lett. **67**, 2670 (1991).